SAR imaging using multidimensional continuous wavelet transform

M. Tria, Jean-Philippe Ovarlez, L. Vignaud, J. Castelli, M. Benidir

SAR IMAGING USING MULTIDIMENSIONAL CONTINUOUS WAVELET TRANSFORM

M. Tria[†‡]*, J-Ph Ovarlez*[‡]*, L. Vignaud*[‡]*, J. Castelli*[‡] *and M. Benidir*[†]

† ONERA, DEMR, BP 72, 92322 Chatillon, France

‡ L.S.S. (UMR 8506), Supelec, 3 rue Joliot Curie, 91192 Gif-sur-Yvette cedex, France

email: tria@onera.fr, ovarlez@onera.fr, vignaud@onera.fr, castelli@onera.fr, benidir@lss.supelec.fr

ABSTRACT

Usually, in radar imaging, we suppose that the reflectors respond the same way regardless of the angle from which they are viewed and have the same properties within the emitted frequency bandwidth. Nevertheless, new capacities in SAR imaging (large bandwidth, large angular excursions of analysis) makes this assumption obsolete. The original application of the multidimensional continuous wavelet transform method in SAR imaging allows to highlight the frequency and angular behavior of these reflectors. This paper discusses the utility of the wavelet transform in SAR imaging for extracting from real targets some essential features allowing to distinguish objects that belong to different classes.

KEY WORDS

SAR Imaging, Wavelet Transform, Time-Frequency Distribution, Feature extraction, Identification, Recognition, Automatic Target Recognition (ATR).

1. GENERAL DESCRIPTION OF THE PROBLEM

The radar imaging process [8] consists in analyzing the reflected signal $H(\vec{k})$ collected by a moving radar (figure 1) and to form the spatial repartition $I(\vec{r})$ of the bright scatterers which reflect a part of the emitted radar signal [9, 10, 11]. The wave vector $\vec{k}$ is related to the emitted frequency f and to the direction θ of radar illumination by relations :

$$\begin{aligned} \left|\vec{k}\right| &= \frac{2f}{c} \\ \theta &= \arg(\vec{k}) \end{aligned}$$

where c is the speed of light, and the extra-factor 2 accounts for the round trip delay (in time) of the signal.

If the object is illuminated using a broad-band signal and/or for and a large angular extent, it is realistic to consider that the amplitude of the reflectors show a dependence on frequency and on aspect angle. Such amplitude variation of scatterers has to be highlighted in order to see if this variation is potentially interpretable in terms of target characteristics.

Considering this amplitude variation, the spatial repartition of reflectors $I(\vec{r})$ must depend on the wave vector $\vec{k}$ and must now be noted $I(\vec{r},\vec{k})$.

The quantity $I(\vec{r},\vec{k})$ is, in fact, the energy distribution of the reflected signal $H(\vec{k})$ in the hyperplan $(\vec{r},\vec{k})$ and will be seen, next, as "extended images" relative to the spatial repartition $I(\vec{r})$.

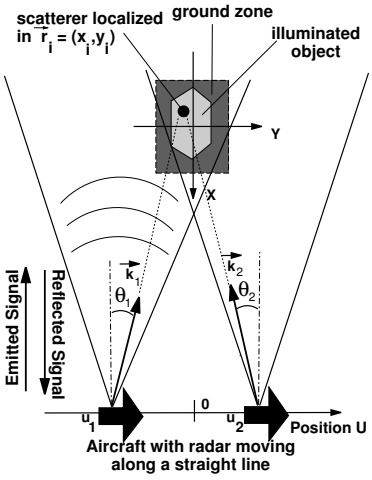

Figure 1: *A reflector, viewed at two different illumination angles in SAR-stripmap mode*

The next section is devoted to the construction of these distributions $I(\vec{r},\vec{k})$ using the time-frequency analysis and the physical group theory.

First, general distributions are constructed based on a hermitian and bilinear form of the reflected signal $H(\vec{k})$. Then, to overcome some drawbacks generated by this construction, we focus on the construction of regularized distributions that will introduce the wavelet transform.

2. EXTENDED RADAR IMAGING

Time-frequency analysis and the physical group theory allow to construct extended radar images [1, 2, 3, 4]. The dimension of these images, called hyperimages, is the product of the dimension of the vector $\vec{r}$ by the dimension of the vector $\vec{k}$.

The principle of the extended radar imaging [1] is based on a physical group of transformations, the similarity group $\mathscr{S}$. This is acting on physical variables $\vec{r}$ and $\vec{k}$ by rotations $\mathscr{R}_\theta$, dilations a in length (or time) and translations $\delta\vec{r}$ according to :

$$\begin{array}{ccc} \vec{r} & \rightarrow & \vec{r}' = a\mathscr{R}_\theta \vec{r} + \delta\vec{r} \\ \downarrow & & \downarrow \\ \vec{k} & \rightarrow & \vec{k}' = a^{-1}\mathscr{R}_\theta \vec{k}. \end{array} \quad (1)$$

The transformation law of the reflected signal $H(\vec{k})$ and its extended image $I(\vec{r},\vec{k})$ in a change of such a reference system is therefore given by :

$$\begin{array}{ccc} H(\vec{k}) & \rightarrow & H'(\vec{k}) = a\, e^{-2i\pi\vec{k}.\delta\vec{r}} H\left(a\mathscr{R}_\theta^{-1}\vec{k}\right) \\ \downarrow & & \downarrow \\ I(\vec{r},\vec{k}) & \rightarrow & I'(\vec{r},\vec{k}) = I\left(a^{-1}\mathscr{R}_\theta^{-1}(\vec{r}-\delta\vec{r}), a\mathscr{R}_\theta^{-1}\vec{k}\right). \end{array} \quad (2)$$

2.1 A general formulation of the extended images

To construct the energy distribution $I(\vec{r},\vec{k})$, a first approach consists in representing it as a hermitian and bilinear form of the signal $H(\vec{k})$ reflected by the target :

$$I(\vec{r},\vec{k}) = \int\int K(\vec{k}_1,\vec{k}_2;\vec{r},\vec{k}) H(\vec{k}_1) H^*(\vec{k}_2)\, d\vec{k}_1\, d\vec{k}_2, \quad (3)$$

where the kernel $K(\vec{k}_1,\vec{k}_2;\vec{r},\vec{k})$ is supposed to be hermitian. This kernel is not known but can be determined with some physical constraints made on the distribution $I(\vec{r},\vec{k})$:

- The distribution can satisfy the property of covariance by the similarity group $\mathscr{S}$ given by (2),
- The distribution $I(\vec{r},\vec{k})$ can be seen, in $\mathbf{R}^2$, as a spatial density (for a given $\vec{k}$). Then , the distribution, has to be positive. Its integral on some surface $\mathscr{D}$ can, therefore, be interpreted as the RCS (Radar Cross Section) contribution $\sigma_{\mathscr{D}}(\vec{k})$ of all the reflectors contained in $\mathscr{D}$:

$$\sigma_{\mathscr{D}}(\vec{k}) = \int_{\mathscr{D}} I(\vec{r},\vec{k})\, d\vec{r}. \quad (4)$$

- If $\mathscr{D}$ represents the whole plan, the distribution can respect the well known marginal property :

$$\int I(\vec{r},\vec{k})\, d\vec{r} = \left|H(\vec{k})\right|^2. \quad (5)$$

- The energy conservation between the distribution space and the reflected signal space leads to an important relation (Moyal formula) which connects the inner product between two given reflected signals H_1 and H_2 and their associated distributions I_1 and I_2 :

$$\left|\int H_1(\vec{k}) H_2^*(\vec{k})\, d\vec{k}\right|^2 = \int\int I_1(\vec{r},\vec{k}) I_2^*(\vec{r},\vec{k})\, d\vec{r} d\vec{k}. \quad (6)$$

The time-frequency analysis has shown that no distribution can satisfy all these properties. For example, the property (6) does not always allow to obtain a distribution everywhere positive, which is inconsistent with the RCS nature of the distribution given by (4) or (5).

To overcome this drawback, it is possible to construct a regularized form of these distributions obtained by smoothing the general distribution given by (3). These regularized distributions verify the constraints (2), (4) and (6) but not the marginalisation property (5). The construction of these extended images which introduces the wavelet transform, is developed in the next section.

2.2 Construction of the extended images by Wavelet transform

Let $\phi(k,\theta)$ be a mother wavelet supposed to represent the signal reflected by a reference target. The associated distribution $I_\phi(\vec{r},\vec{k})$ is supposed to be well located around the spatial origin $\vec{r} = \vec{0}$ and $(k,\theta) = (1,0)$. For example, one can use a two-dimensional separate gaussian function :

$$\phi(k,\theta) \quad = \quad e^{-(\frac{k-1}{\sigma_k})^2} \cdot e^{-(\frac{\theta}{\sigma_\theta})^2}$$

where the two free parameters σ_k and σ_θ control the spread in frequency and in angular domain and play on interrelated resolutions in spatial domain $\vec{r} = (x,y)$, frequency and angle.

By the action of the group $\mathscr{S}$, a family of wavelet bases $\Psi_{\vec{r}_0,\vec{k}_0}(\vec{k})$ can be generated from the mother wavelet $\phi(k,\theta)$ according to :

$$\begin{aligned} \Psi_{\vec{r}_0,\vec{k}_0}(\vec{k}) &= \frac{1}{k_0} e^{-2i\pi\vec{k}.\vec{r}_0} \phi\left(\frac{1}{k_0}\mathscr{R}_{\theta_0}^{-1}\vec{k}\right) \\ &= \frac{1}{k_0} e^{-2i\pi\vec{k}.\vec{r}_0} \phi\left(\frac{k}{k_0}, \theta-\theta_0\right). \end{aligned} \quad (7)$$

A regularized distribution $\tilde{I}(\vec{r}_0,\vec{k}_0)$ can be constructed by smoothing the general distribution $I(\vec{r},\vec{k})$ given by (3).
And using Moyal formula (6), covariance property (2) with $H_1(\vec{k}) = H(\vec{k})$, $H_2(\vec{k}) = \Psi_{\vec{r}_0,\vec{k}_0}(\vec{k})$, $I_1 = I_H$ and $I_2 = I_\phi$, we obtain :

$$\begin{aligned} \tilde{I}(\vec{r}_0,\vec{k}_0) &= \iint I_H(\vec{r},\vec{k}) \times \\ &\quad I_\phi^*\left(k_0\mathscr{R}_{\theta_0}^{-1}(\vec{r}-\vec{r}_0), \frac{1}{k_0}\mathscr{R}_{\theta_0}^{-1}\vec{k}\right) d\vec{r} d\vec{k} \\ &= \left|\int H(\vec{k}) \frac{1}{k_0} e^{2i\pi\vec{k}.\vec{r}_0} \phi^*\left(\frac{1}{k_0}\mathscr{R}_{\theta_0}^{-1}\vec{k}\right) d\vec{k}\right|^2 \end{aligned} \quad (8)$$

The right hand side is nothing but the wavelet coefficient $C(\vec{r}_0,\vec{k}_0)$ which is introduced as the invariant scalar product of the group $\mathscr{S}$ between the reflected signal H and each element $\Psi_{\vec{r}_0,\vec{k}_0}$ of the wavelet basis :

$$\begin{aligned} C(\vec{r}_0,\vec{k}_0) &= \int H(\vec{k}) \Psi^*_{\vec{r}_0,\vec{k}_0}(\vec{k})\, d\vec{k} \\ &= \int_0^{2\pi} d\theta \int_0^{+\infty} k H(k,\theta) \Psi^*_{\vec{r}_0,\vec{k}_0}(\vec{k})\, dk. \end{aligned} \quad (9)$$

The reconstruction property allows to recover the signal with the knowledge of its wavelet coefficients :

$$H(\vec{k}) = \frac{1}{\kappa(\phi)} \int d\vec{r}_0 \int C(\vec{r}_0, \vec{k}_0)\, \Psi_{\vec{r}_0,\vec{k}_0}(\vec{k})\, d\vec{k}_0, \qquad (10)$$

where $\kappa(\phi)$ is the admissibility coefficient defined as :

$$\kappa(\phi) = \int \frac{|\phi(\vec{k})|^2}{k^2}\, d\vec{k} \; < \infty. \qquad (11)$$

• **Interpretation of the distribution $I(\vec{r},\vec{k})$:**

Let us Rewritten $I(\vec{r},\vec{k}) \equiv I(x,y;f,\theta)$: for each frequency f_o and each angle of radar illumination θ_o, $I(x,y;f_o,\theta_o)$ represents a spatial repartition of reflectors which respond at this frequency and this angle.

Inversely, for each reflector located at $\vec{r}_o = (x_o, y_o)$, we can extract its feature $I(x_o,y_o;f,\theta)$ in frequency f and in angular θ. This is this aspect that we decided to point out in order to see if this quantity can be interpretable in terms of target characteristics.

To analyze this 4D structure, a visual display interface called *i4D* [7] has been developed and allows to carry out an interactive and dynamic analysis.

3. EXPERIMENTAL RESULTS

We present, here, some results of SAR imaging using wavelets. We focus on the fact that each reflector in the image can be characterized by his own energy distribution in the space (f,θ).

We've chosen to show this energy distribution for reflectors belonging to a long metallic pipe and to a building (figure 2). Concerning the building, we focused on reflectors belonging to the front ridge (relative to the radar's position) and to the roof.

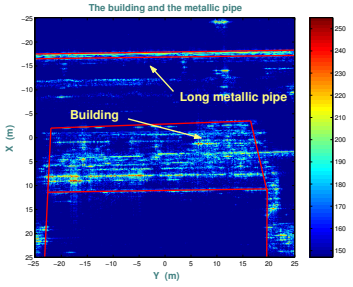

Figure 2: *Pipe and Buiding type target built by classical radar imaging*

In the following figures 3, 4, 5, the image, on the left, represents the spatial repartition of the scatterers at the emitted frequency $f_o = 14.2$ GHz and the illumination angle $\theta_o = 0.89\,^\circ$. In this image, we select a pixel (with the curser) and the energy repartition in the (f,θ) space corresponding to this pixel is pointed out in the right picture.

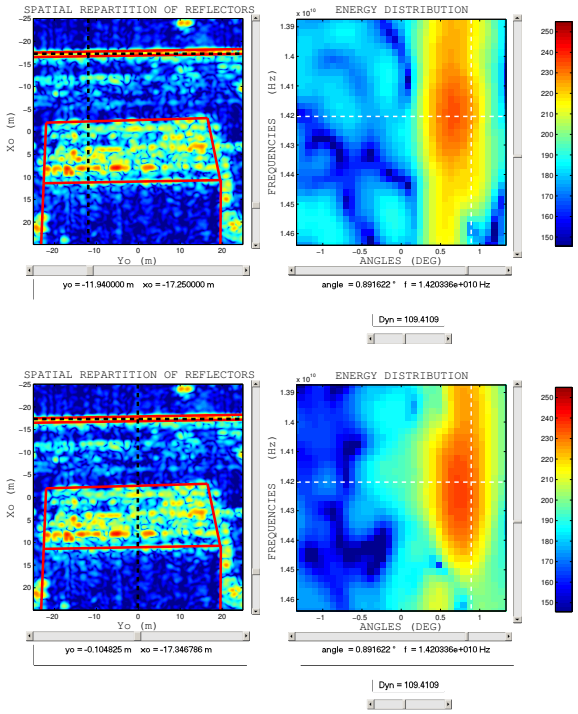

Figure 3: *Energy Distribution $I(x_o,y_o;f,\theta)$ of 2 given reflector respectively located at ($x_o = -17.25$ m,$y_o = -11.94$ m) and ($x_o = -17.34$ m,$y_o = -0.10$ m)* ***on the long metallic pipe****: the energy spreads in a very restricted angular domain and not the same way on the frequency band. It was observed for most reflectors belonging to the pipe.*

4. CONCLUSIONS

The multidimensional wavelet transform analysis for the SAR imaging can highlight some characteristics of the reflectors that the classical SAR imaging can not do. Moreover, we've seen in the previous examples (figures 3, 4 and 5) that, the reflectors belonging to the same "structure" (either the pipe, or the ridge of the building, or the roof of the building) have a similar response in frequency and angle. Inversely, the response differs significatively from one structure to the other. The geometry [13],[14] and the material composition of these structures can influence these distinctions.

This is why, the goal, now, is to see if theses characteristics can be interpretable in terms of target feature extraction. An extension of the studies to other real targets at different frequency bands and various angular extension is in project. Indeed, even if the computation of wavelet transform in SAR imaging needs high memory, it is inexpensive in time even for real data.

A first step that can be proposed is to have, in the same image, two pieces of information : the localization of the reflectors, and the energy characteristics. This last information can be represented in the image, for example with a color system coding : each color will represent a coefficient obtained by maximization of the correlation between the energy distribution and a set of given basis functions. This step has to be

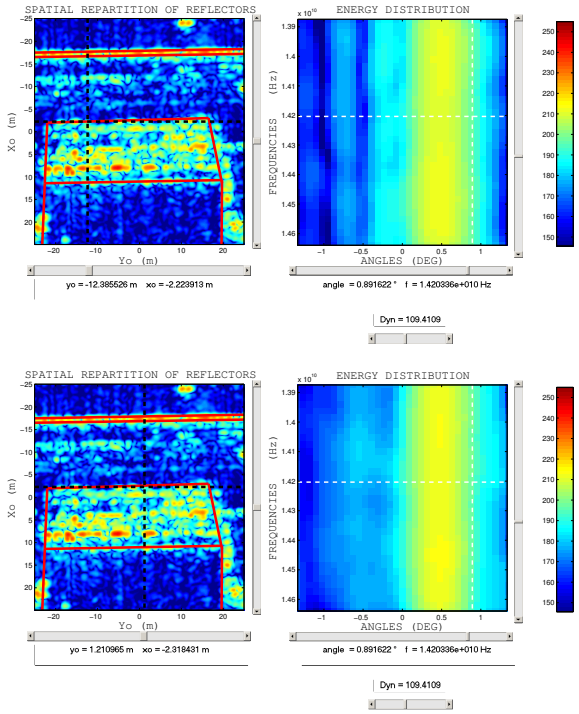

Figure 4: *Energy Distribution $I(x_o, y_o; f, \theta)$ of 2 given reflector respectively located at ($x_o = -2.22$ m,$y_o = -12.38$ m) and ($x_o = -2.91$ m,$y_o = 1.21$ m)* ***on the front ridge of the building****: the energy spreads in a very restricted angular domain and seems not depend on the emitted frequency. It was observed for most of the scatterers belonging to this ridge.*

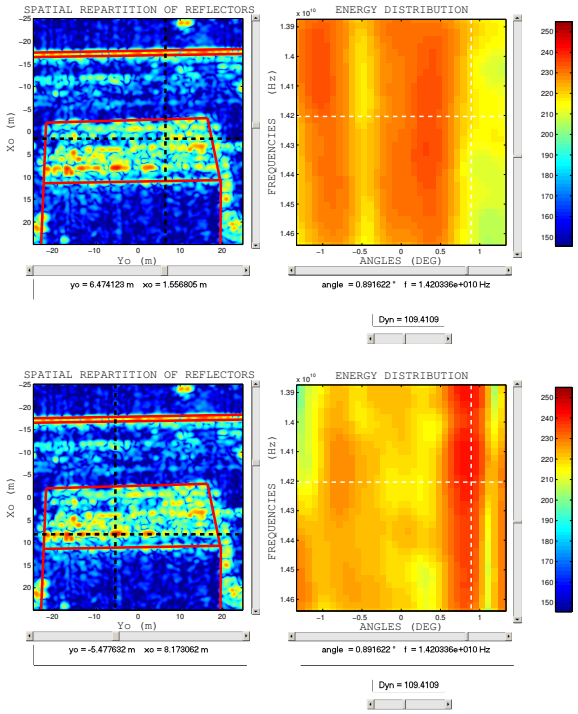

Figure 5: *Energy Distribution $I(x_o, y_o; f, \theta)$ of 2 given reflector respectively located at ($x_o = 1.55$ m,$y_o = 6.47$ m) and ($x_o = 8.17$ m,$y_o = -5.47$ m)* ***on the roof of the building****: the energy almost spreads all over the space (f, θ) but not uniformly. It was observed for a non-negligible number of reflectors on the roof of the building.*

integrated on an automatic process. The purpose is to identify the constituents of a target for a better interpretation of it.

REFERENCES

[1] J. Bertrand P. Bertrand and J.P. Ovarlez, Frequency Directivity Scanning in Laboratory Radar Imaging, *Int. J. of Imaging Systems and Technology*, **5** (1994), 39-51.

[2] J.P. Ovarlez L. Vignaud J.C. Castelli M. Tria and M. Benidir, Analysis of SAR Images by Multidimensional Wavelet Transform, *IEE-Radar, Sonar and Navigation- Special Issue On Time-Frequency Analysis for Synthetic Aperture Radar and Feature Extraction*, **150**(4) (august 2003), 234-241.

[3] J.P. Ovarlez L. Vignaud J.C. Castelli M. Tria and M. Benidir, Analysis of SAR Images by Multidimensional Wavelet Transform, 5^{th} *IASTED International Conference On Signal & Image Processing*, (August 13-15, 2003), Honolulu.

[4] J. Bertrand P. Bertrand and J.P. Ovarlez, Dimensionalized Wavelet Transform with Application to Radar Imaging, *Proc. IEEE-ICASSP* (May 1991), Toronto, Canada.

[5] D.L. Mensa, *High Resolution Radar Imaging*, Artech House (1981), USA.

[6] J. Bertrand and P. Bertrand, The Concept of Hyperimage in Wide-Band Radar Imaging, *IEEE Trans. Geosc. Remote Sensing*, **34** (1996), 1144-1150.

[7] J.C. Castelli and G. Bobillot, I4D : A New Approach to RCS Imaging Analysis, *Proc. AMTA* (Nov. 1997) Boston, USA.

[8] W.G. Carrara R.S. Goodman and R.M. Majewski, *Spotlight Synthetic Aperture Radar*, Artech House, Boston, London.

[9] M. Soumekh, *Fourier Array Imaging*, PTR Prentice Hall (1994), Englewood Cliffs.

[10] M. Soumekh, *Synthetic Aperture Radar Signal Processing*, John Wiley & Sons, Inc.

[11] P.T. Gough D.W. Hawkins, Unified Framework for Modern Synthetic Aperture Imaging Algorithms, *Int. J. of Imaging Systems and Technology*, **8** (1997), 343-358.

[12] J.M. Boutry, ONERA Airborne SAR Facilities, *2nd International Airborne Remote Sensing Conference* (June 1996), San Francisco, USA.

[13] L.C. Potter D.M. Chiang R. Carrire and M.J. Gerry, A Geometrical Theory of Diffraction (GTD)-Based Parametric Model for Radar Scattering, *IEEE Trans. On Antennas and Propagation*, **43** (Oct. 1995), 1058-1067.

[14] L.C. Potter and R.L. Moses, Attributed Scattering Centers for SAR ATR, *IEEE Trans. On Image Processing*, **6** (Jan. 1997), 79-91.